SOON CHUN HYANG UNIVERSITY HOSPITAL CHEONAN

Experimental and clinical study of flap monitoring with analysis of clinical course of the flap using Infrared thermal camera

Hwan Jun Choi

Department of Plastic & Reconstructive surgery, College of medicine,

Soonchunhyang University, Cheonan, South Korea

Abstract

- Flap surgery is a common method used to cover defects following tumor ablation, trauma, or infection. However, insufficient vascularity in the transferred flap can lead to flap necrosis and failure. Proper postoperative monitoring is essential to prevent these complications. Recently, research has explored the use of infrared thermal imaging in plastic surgery, leading to its clinical application.
- This study comprises two separate parts: an in vivo experimental study and a clinical study. In this study, 28 rats underwent reverse McFarlane flap surgery, and their flaps were analyzed using a FLIR thermal imaging camera seven days post-surgery. Additionally, thermal images of flaps were taken on postoperative days 0, 1, 2, 3, and 7 in 22 patients. This study focused on temperature differences between normal skin and the perforator compared to the average flap temperature.
- Results showed that the temperature difference was higher in the necrosis group and increased over time in cases of total necrosis. A lower perforator temperature compared to the flap's average indicated vascular compromise, potentially leading to flap failure. The FLIR camera, being contact-free and convenient, shows promise for understanding and inferring the clinical progression of flaps in postoperative monitoring.

Methods

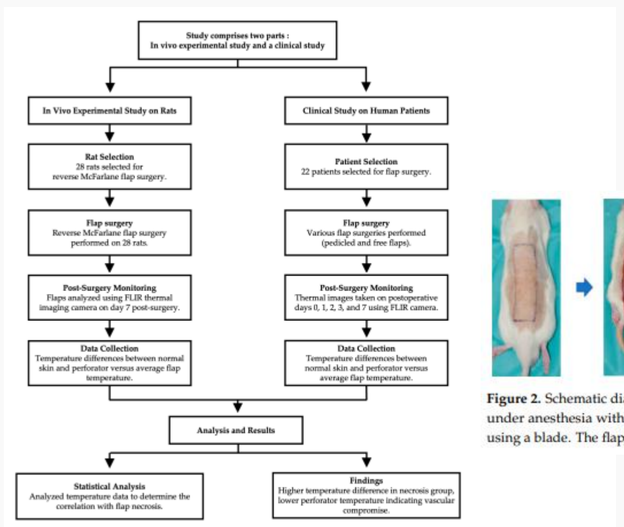

Figure 1. Study design overview. The diagram illustrates the structure and flow of the in vivo experimental study and the clinical study.

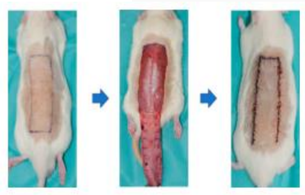

Figure 2. Schematic diagram of surgical procedures. Incisions were made on the back of the mouse under anesthesia with isoflurane, and a 3 × 9 cm sized reverse McFarlane skin flap was elevated using a blade. The flap was immediately closed with sutures using 4-0 nylon.

Results

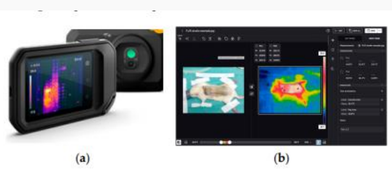

Figure 3. FLIR camera and thermal analysis software. (**a**) The FLIR C5 camera (Teledyne FLIR LLC, Wilsonville, OR, USA) has two cameras—a thermal imager (160 × 120 pixels) and 5-megapixel visual camera (640 × 480 pixels). (**b**) FLIR Thermal Studio software (Teledyne FLIR LLC, Wilsonville, OR, USA) is displayed on the right. It is used to analyze thermal images, which allows the user to identify the temperature of a specific point or area on the image and calculate the temperature difference.

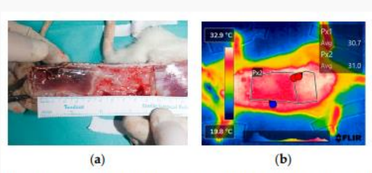

Figure 4. Analysis of flap necrosis in rat models. (**a**) After euthanization of the rats, the total flap and necrotic areas were measured with distinguishment of flap viability. (**b**) The thermal images were captured by FLIR camera, indicating the necrosis area (colored red), which shows a drop in temperature compared to the viable area (colored white). The temperature difference between the total flap area and necrotic area was calculated by using infrared thermal software.

Table 1. Thermal analysis of rat models.

Flap Models (n = 28)	POD 3	POD 7
Necrotic area/total flap ratio (%)	24.4	27.5
Temperature difference between total flap and necrotic area	0.800	0.792

Abbreviations: POD, postoperative day.

Table 2. Summary of paired t-test results.

Statistic	Value
t-value	0.084
p-value	0.934

Table 3. Summary of regression analysis results.

Dependent Variable	Coefficient	Std. Error	t-Value	p-Value
POD3 Necrotic Area Temp				
Intercept	28.069	4.663	6.020	0.000
Before Flap Temp	0.149	0.141	1.057	0.300
POD7 Necrotic Area Temp				
Intercept	27.592	5.045	5.469	0.000
Before Flap Temp	0.156	0.153	1.024	0.315

Abbreviations: Std. error, standard error; POD, postoperative day; Temp, temperature.

Table 4. Summary of GLMM results.

Variable	Coefficient	Std. Error	z-Value	p-Value	95% CI Lower	95% CI Upper
Intercept (POD3)	0.274	1.126	0.243	0.808	−1.934	2.481
Before Flap Temp	−0.040	0.023	−1.734	0.083	−0.085	0.005
POD3 Total Flap Temp	1.007	0.031	32.568	0.000	0.946	1.068
Intercept (POD7)	0.003	0.881	0.003	0.997	−1.724	1.730
Before Flap Temp	−0.004	0.001	−2.988	0.003	−0.006	−0.001
POD7 Total Flap Temp	0.980	0.025	39.099	0.000	0.931	1.029

Abbreviations: GLMN, generalized linear mixed models; Std. error, standard error; CI, confidence interval; POD, postoperative day; Temp, temperature.

Table 5. Patients demographics.

No. of Patient	Sex	Age	Location	Flap	Flap Type	Flap Necrosis
1	M	61	Lt. ankle	ALT free flap	Free flap	No necrosis
2	F	27	Scalp	ALT free flap	Free flap	No necrosis
3	M	16	Lt. ankle	ALT free flap	Free flap	No necrosis
4	M	55	Lt. lower leg	ALT free flap	Free flap	No necrosis
5	M	72	Philtrum	ALT free flap	Free flap	No necrosis
6	F	66	Lt. ankle	ALT free flap	Free flap	No necrosis
7	F	100	Lt. upper eyelid	ALT free flap	Free flap	No necrosis
8	M	60	Lt. foot	ALT free flap	Free flap	Total necrosis
9	M	63	Lt. ankle	ALT free flap	Free flap	No necrosis
10	M	51	Lt. foot	ALT free flap	Free flap	Total necrosis
11	F	70	Rt. foot	ALT free flap	Free flap	No necrosis
12	M	48	Lt. ankle	TDAP free flap → ALT free flap	Free flap	No necrosis
13	F	23	Lt. hand	SCIP free flap	Free flap	No necrosis
14	M	75	Scalp	ALT free flap → vastus lateralis muscle free flap	Free flap	Total necrosis
15	M	81	Nose	Nasolabial fold flap	Pedicled flap	No necrosis
16	M	56	Nose	Nasolabial fold flap	Pedicled flap	No necrosis
17	M	52	Nose	Nasolabial fold flap	Pedicled flap	No necrosis
18	M	91	Nose	Paramedian forehead flap	Pedicled flap	No necrosis
19	M	57	Nose	Paramedian forehead flap	Pedicled flap	No necrosis
20	M	57	Rt. lower leg	ALT pedicled flap	Pedicled flap	No necrosis
21	F	49	Rt. ankle	Peroneal artery perforator-based FC rotation flap	Pedicled flap	Partial necrosis

Abbreviations: Rt, right; Lt, left; ALT, the anterolateral thigh; TDAP, the thoracodorsal artery perforator; SCIP, the superficial circumflex iliac artery perforator; FC, fasciocutaneous.

Table 6. Flap characteristics.

	Necrosis Group (n = 4)
Necrosis type	
Total necrosis	3
Partial necrosis	1
Vascular compromise	
Arterial insufficiency	2
Venous congestion	2

Table 7. Analysis of comparison between non-necrosis group and necrosis group.

	Non-Necrosis (n = 18)	Necrosis (n = 4)	Total Necrosis (n = 3)	Partial Necrosis (n = 1)
Age (years)	57.167	58.75		
Sex				
Male	13	3		
Female	5	1		
Temperature difference (dT) between normal skin and perforator (NS-PF) (°C)				
POD 0	1.817	1.55 (0.484)	1.633 (0.740)	1.3 (0.526)
POD 1	1.533	1.875 (0.434)	2 (0.262)	1.5 (0.842)
POD 2	1.528	2.2 (0.434)	2.467 (0.262)	1.4 (0.842)
POD 3	0.989	2.525 (0.001 *)	2.533 (0.006 *)	2.5 (0.105)
POD 7	0.706	3.5 (<0.001 *)	4 (0.002 *)	2 (0.105)
Temperature difference (dT) between perforator and average of flap (PF-AFP) (°C)				
POD 0	0.539	0.175 (0.118)	0.2	0.1
POD 1	0.35	−0.175 (0.002 *)	−0.2	−0.1
POD 2	0.333	−0.225 (0.003 *)	−0.2	−0.3
POD 3	0.617	−0.375 (<0.001 *)	−0.233	−0.8
POD 7	0.489	−0.225 (<0.001 *)	−0.333	−0.1

Note: Values are expressed as means. The value between the parentheses corresponds to the p-value for statistical significance between the group and the non-necrosis group. * p-value < 0.05. Abbreviations: POD, postoperative day; dT, temperature difference; NS-PF, normal skin–perforator; PF-AFP, perforator–average of flap.

Table 8. NS-PF POD 7 model results.

Variable	Coefficient	p-Value
Sex (male)	0.475	<0.001
Flap type (free flap)	0.185	0.611
Flap type (pedicled flap)	−0.647	0.003
Flap necrosis (necrosis)	2.631	<0.001

Abbreviations: NS-PF, normal skin–perforator.

Table 9. PF-AFP POD 7 model results.

Variable	Coefficient	p-Value
Sex (male)	−0.258	0.088
Flap type (free flap)	−0.070	0.768
Flap type (pedicled flap)	0.093	0.515
Flap necrosis (necrosis)	−0.716	<0.001

Abbreviations: PF-AFP, perforator–average of flap.

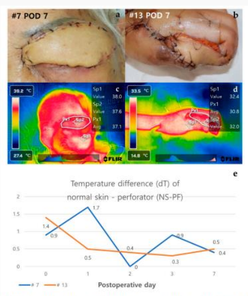

Figure 6. Analysis of cases of non-necrosis group (Case #7 and Case #13). (**a**) Case #7—A 100-year-old female patient underwent reconstruction through ALT free flap after tumor resection due to skin cancer on the left upper eyelid. On POD 7, the flap was maintained stably without any necrosis. (**b**) Case #13—A 23-year-old female patient who underwent SCIP free flap reconstruction after distal finger necrosis due to use of vasopressors. On POD 7, the flap has no necrosis. (**c**,**d**) In the thermal images of POD 7, both flaps have a similar color to the surrounding area except for some margins. (**e**) The graph shows NS-PF decreasing over time. Abbreviations: POD, postoperative day; dT, temperature difference; NS-PF, normal skin–perforator; ALT free flap, the anterolateral thigh free flap; SCIP free flap, the superficial circumflex iliac artery perforator free.

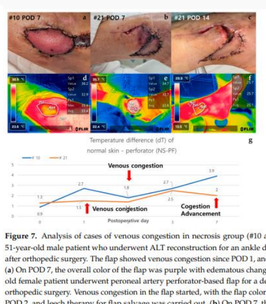

Figure 7. Analysis of cases of venous congestion in necrosis group (#10 and #21). Case #10 is a 51-year-old male patient who underwent ALT reconstruction for an ankle defect that had occurred after orthopedic surgery. The flap showed venous congestion since POD 1, and it gradually worsened. (**a**) On POD 7, the overall color of the flap was purple with edematous change. Case #21—A 49-year-old female patient underwent peroneal artery perforator-based flap for a defect that occurred after orthopedic surgery. Venous congestion in the flap started, with the flap color appearing purple since POD 2, and leech therapy for flap salvage was carried out. (**b**) On POD 7, the distal part of the flap still showed features of congestion, but the central part showed improvement with a lightening of color. (**c**) On POD 14, the necrotic area was demarcated, resulting in distal partial necrosis. (**d**,**e**) In the thermal images of POD 7, both flaps appeared yellow in color as the temperature dropped. (**f**) In the thermal image of Case #21 on POD 14, the difference in temperature decreased in comparison to POD7. (**g**) The graph showed an upward trend over time from the point of venous congestion, but in Case #21, the temperature difference decreased as the congestion improved. Abbreviations: POD, postoperative day; dT, temperature difference; NS-PF, normal skin–perforator; ALT, the anterolateral thigh.

Table 10. T-test results for temperature differences between pedicled and free flaps.

POD	t-Statistic	p-Value
NS-PF POD 0	0.927	0.366
NS-PF POD 1	0.271	0.789
NS-PF POD 2	−0.217	0.831
NS-PF POD 3	−0.656	0.520
NS-PF POD 7	−1.547	0.139
PF-AFP POD 0	1.554	0.138
PF-AFP POD 1	−0.054	0.957
PF-AFP POD 2	0.326	0.748
PF-AFP POD 3	0.068	0.946
PF-AFP POD 7	0.610	0.550

Abbreviations: POD, postoperative day; NS-PF, normal skin–perforator; PF-AFP, perforator–average of flap.

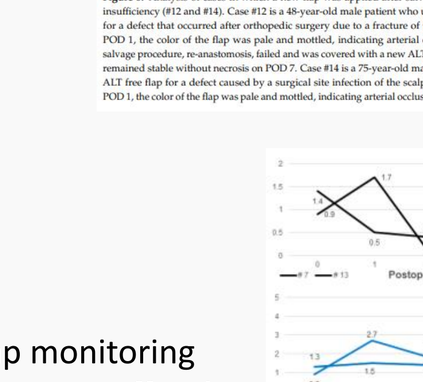

Figure 5. Mean temperature differences (NS−PF and PF−AFP) with 95% confidence intervals across different flap necrosis types. (**a**) Mean NS−PF temperature difference with 95% confidence intervals across different flap necrosis types. (**b**) Mean PF−AFP temperature difference with 95% confidence intervals across different flap necrosis types. Abbreviations: NS−PF, normal skin−perforator; PF−AFP, perforator−average of flap; CI, confidence intervals.

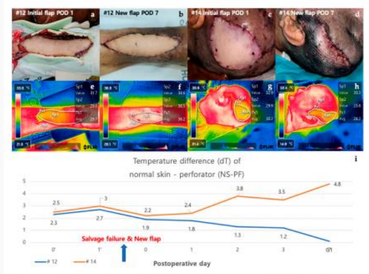

Figure 8. Analysis of cases in which a new flap was applied after salvage procedure for arterial insufficiency (#12 and #14). Case #12 is a 48-year-old male patient who underwent TDAP free flap for a defect that occurred after orthopedic surgery due to a fracture of the left distal tibia. (**a**) On POD 1, the color of the flap was pale and mottled, indicating arterial occlusion of the flap. The salvage procedure, re-anastomosis, failed and was covered with a new ALT free flap. (**b**) The new flap remained stable without necrosis on POD 7. Case #14 is a 75-year-old male patient who underwent ALT free flap for a defect caused by a surgical site infection of the scalp. (**c**) As with Case #12 on POD 1, the color of the flap was pale and mottled, indicating arterial occlusion of the flap. The salvage

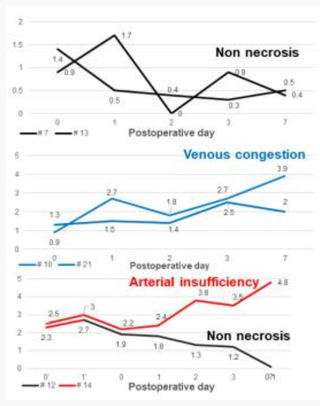

Conclusion

- Numerous studies are investigating flap monitoring using infrared thermal imaging. FLIR cameras offer the benefits of being non-invasive and highly convenient. While further research is necessary before FLIR cameras can serve as definitive indicators for vascular compromise during flap monitoring, they can effectively function as auxiliary tools for assessing and predicting the overall clinical progression of flaps.
- This study introduces a novel method for flap monitoring via infrared thermography by analyzing the temperature differential between the perforator area and the average flap temperature, demonstrating significant potential for enhancing the flap monitoring process.

Reference →